

# Processing and Microstructures of Cr-Ta and Cr-Ta-Mo Composites Reinforced by the Cr<sub>2</sub>Ta Laves Phase<sup>\*</sup>

Dai-Feng Wang

Materials Science and Engineering Department, The University of Tennessee, Knoxville, TN 37996-2200

Email: dwang@utk.edu; Telephone: (865) 974-0645; Fax: (865) 974-4115

Peter K. Liaw

Materials Science and Engineering Department, The University of Tennessee, Knoxville, TN 37996-2200

Email: pliaw@utk.edu; Telephone: (865) 974-6356; Fax: (865) 974-4115

Chain T. Liu

Metals and Ceramics Division, Oak Ridge National Laboratory, Oak Ridge, TN 37831

Email: liuct@ornl.gov; Telephone: (865) 574-4459; Fax: (865) 574-4066

Easo P. George

Metals and Ceramics Division, Oak Ridge National Laboratory, Oak Ridge, TN 37831

and

Materials Science and Engineering Department, The University of Tennessee, Knoxville, TN 37996-2200

Email: georgeep@ornl.gov; Telephone: (865) 574-5085; Fax: (865) 576-3881

## Abstract

The Cr-Ta alloy with an eutectic structure has a good combination of high strength and oxidation resistance at elevated temperatures up to 1,200°C. It is an ideal candidate for ultrahigh-temperature applications. However, the material shows low ductility and fracture toughness at room temperature. An effective way to improve the ductility and fracture toughness is to obtain an aligned microstructure of eutectic Cr-based alloys, using a directional-solidification (DS) process, in which the feed materials with eutectic compositions are preferred. In the present work, a quantitative technique was employed to assist in monitoring and controlling the composition of the Cr-based alloys throughout the processing stages at elevated temperatures. A colony structure related to the instable liquid/solid interface was observed in a DS Cr-Ta sample. A possible eutectic area was probed in the Cr-Mo-Ta system, which could facilitate the development of well-aligned lamellar structures by DS.

---

<sup>\*</sup> Research sponsored by the Fossil Energy Advanced Research and Technology Development (AR&TD) Materials Program, U. S. Department of Energy, under subcontract, 11X-SP173V, to the University of Tennessee, and by the AR&TD Materials Program, under contract with DE-AC05-000R22725 with UT-Battelle, LLC.

## Introduction

The  $\text{Cr}_2\text{X}$  ( $\text{X} = \text{Ti, Hf, Zr, Nb, Ta, etc.}$ ) Laves-phase alloys are candidate materials for applications at temperatures greater than  $1,200^\circ\text{C}$ , because these alloys have good oxidation resistance and strength at elevated temperatures [1-12]. However, these alloys are very brittle at room ( $24^\circ\text{C}$ ) and moderately high temperatures (approximate  $400$  to  $800^\circ\text{C}$ ), which prohibits their commercial applications as structural materials. One of the potential solutions to overcome the brittleness of Laves-phase alloys is to fabricate *in situ* composites reinforced by Laves phases in a relatively ductile matrix [13-20]. The presence of a  $\text{Cr-Cr}_2\text{Ta}$  eutectic reaction provides a good opportunity for the formation of the  $\text{Cr}$  solid solution alloy reinforced with the  $\text{Cr}_2\text{Ta}$  Laves phase [21]. The  $\text{Cr-Cr}_2\text{Ta}$  alloy has a high melting point greater than  $1,700^\circ\text{C}$ , and the Laves phase has an ordered crystal structure so that it shows excellent mechanical properties at elevated temperatures. In addition, the  $\text{Cr}$  matrix phase exhibits some ductility, which is greater than the  $\text{Cr}_2\text{Ta}$  Laves phase at room temperature [3, 22], and good oxidation resistance at high temperatures. The mechanical properties of the  $\text{Cr}$  matrix can be improved by the mechanical treatment and alloying-element additions [22-24]. Thus, the  $\text{Cr}$  solid solution matrix composite reinforced by Laves phases makes the material attractive. Our previous research showed that aligned lamellar structures obtained by directional solidification (DS) using a High-Temperature Optical-Floating-Zone Furnace could improve the strength and toughness of the  $\text{Cr-Cr}_2\text{Ta}$  *in situ* composites [25].

Eutectic compositions of the  $\text{Cr}$ -based alloys are critical for obtaining well-aligned lamellar structures using DS. It is worth noting that the published data of the eutectic composition of the  $\text{Cr-Ta}$  binary system range from 9.8 atomic percent (at. %)  $\text{Ta}$  [10] to 13 at. %  $\text{Ta}$  [19], and molybdenum alloying is thought to be capable of solid-solution hardening of the  $\text{Cr}$ -rich phase [26]. To achieve the desired compositions, proper masses of the raw materials are calculated prior to processing. However, there is a large difference between the melting points of  $\text{Cr}$  and  $\text{Ta}$ , and the boiling point of  $\text{Cr}$  is lower than that of  $\text{Ta}$ . Thus, the vaporization of chromium during processing, especially at the initial stage, should be taken into account. Moreover, a considerable weight loss due to the  $\text{Cr}$  evaporation could occur during directional solidification, where the molten alloy is exposed to ultrahigh temperatures for long times. Such fluctuations in the compositions of the  $\text{Cr}$ -based materials would have influence on the final microstructures of the DS materials.

## Experimental

High-purity  $\text{Cr}$ ,  $\text{Ta}$ , and  $\text{Mo}$  chips were used as charge materials in order to avoid deleterious effects of impurities on the microstructures and mechanical properties of the alloys. The nominal compositions of the alloys studied are shown in Table 1. Unless specified otherwise, the compositions mentioned are in at. % hereafter. Button-shaped samples of the alloy were obtained by arc-melting in argon. Every sample was inverted and remelted for eight to ten times in order to improve the homogeneity of the microstructure and chemical composition of the alloy. Then cylindrical ingots with a length of 60 mm and a diameter of 9 mm were obtained by drop-casting. Selected samples were further processed by directional solidification in a flowing argon atmosphere using a High-Temperature Optical-Floating-Zone Furnace. Details of the directional-solidification processing can be found elsewhere [25]. A quantitative technique was employed to track the composition deviations during processing [27]. At each processing stage, weight loss was carefully measured and tracked for the ingot (Figure 1). The evaporation of the chromium was assumed to be the only source of the weight loss, and the corresponding actual composition was calculated and recorded for tracking purposes, as illustrated in Figure 1. The actual masses of the alloying elements prior to each processing stage except the raw materials were calculated by the derived actual composition of the last stage, and then were converted to concentrations in atomic percentages to reflect the composition deviations during processing (Figure 1).

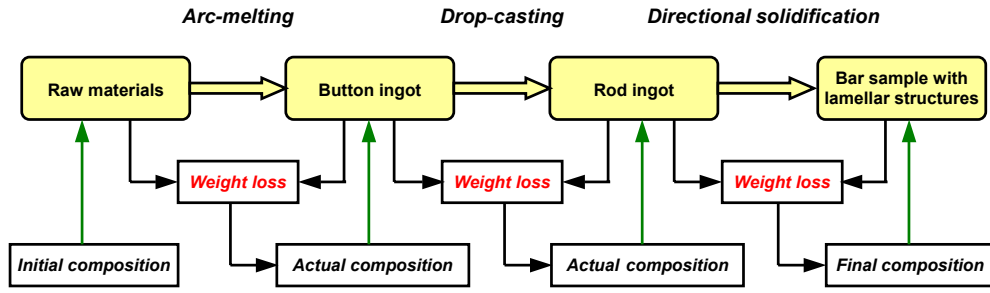


Figure 1 Composition monitoring and tracking during different processing stages.

For a binary Cr-X alloy system, the actual concentration of an alloying element, X, after a certain processing stage was calculated by the following equation:

$$X \text{ at. \%} = \frac{W_X/M_X}{W_X/M_X + (W_{Cr} - \Delta W)/M_{Cr}} \times 100\% \quad (1)$$

where,  $M_X$  and  $M_{Cr}$  are the atomic masses of the alloying elements, X and Cr, respectively,  $W_X$  and  $W_{Cr}$  are the weights of X and Cr prior to the processing stage, and  $\Delta W$  is the weight loss that equals the sum of  $W_X$  and  $W_{Cr}$  minus the ingot weight. The actual composition in a ternary Cr-X-Y alloy system can be calculated in a similar way, as shown in Equation 2:

$$\begin{cases} X \text{ at. \%} = \frac{W_X/M_X}{W_X/M_X + W_Y/M_Y + (W_{Cr} - \Delta W)/M_{Cr}} \times 100\% \\ Y \text{ at. \%} = \frac{W_Y/M_Y}{W_X/M_X + W_Y/M_Y + (W_{Cr} - \Delta W)/M_{Cr}} \times 100\% \end{cases} \quad (2)$$

where,  $M_Y$  and  $W_Y$  are the atomic mass and weight of the ternary alloying element, Y, respectively. Following the processing, the microstructures of the samples were examined using optical microscopy (OM).

Table 1 Nominal compositions of the Cr-Ta and Cr-Ta-Mo alloys (at. %)

Alloy system	Nominal compositions
Cr-Ta	Cr-9.6Ta
Cr-Ta-Mo	Cr-9.7Ta-1.0Mo, Cr-9.7Ta-3.0Mo, Cr-9.7Ta-5.0Mo, Cr-10.7Ta-5.0Mo, Cr-11.7Ta-3.0Mo, Cr-13.7Ta-1.0Mo

## Results and discussion

### 1. Composition deviations of the Cr-based alloys during processing

The compositions of the Cr-Ta and Cr-Ta-Mo samples throughout various processing stages are calculated by Equations 1 and 2, and are listed in Table 2. Note that surplus chromium was added prior to arc-melting to compensate for the Cr

evaporation, and the initial Ta and/or Mo concentrations were lower than the nominal values. It was found that for the drop-cast Cr-based alloys, the actual composition could be controlled to a level very close to the nominal value. However, a more significant increase in the Ta content occurred in the DS sample (Figure 2), which can be attributed to the long-time exposure of the sample to ultrahigh temperatures of about 1,800 °C during DS processing.

Table 2 Composition deviations during different stages of the processing (at. %)

Nominal composition	Processing stages			
	Raw materials	Arc-melting	Drop-casting	Directional solidification
Cr-9.6Ta	Cr-9.37Ta	Cr-9.46Ta	Cr-9.49Ta	Cr-9.60Ta
Cr-9.7Ta-1.0Mo	Cr-9.58Ta-0.99Mo	Cr-9.64Ta-0.99Mo	Cr-9.70Ta-1.00Mo	--
Cr-9.7Ta-3.0Mo	Cr-9.60Ta-2.97Mo	Cr-9.65Ta-2.99Mo	Cr-9.67Ta-2.99Mo	--
Cr-9.7Ta-5.0Mo	Cr-9.60Ta-4.95Mo	Cr-9.67Ta-4.99Mo	Cr-9.71Ta-5.01Mo	--
Cr-10.7Ta-5.0Mo	Cr-10.63Ta-4.96Mo	Cr-10.73Ta-5.00Mo	Cr-10.76Ta-5.02Mo	--
Cr-11.7Ta-3.0Mo	Cr-11.56Ta-2.93Mo	Cr-11.66Ta-2.99Mo	Cr-11.69Ta-3.00Mo	--
Cr-13.7Ta-1.0Mo	Cr-13.55Ta-0.99Mo	Cr-13.70Ta-1.00Mo	Cr-13.75Ta-1.00Mo	--

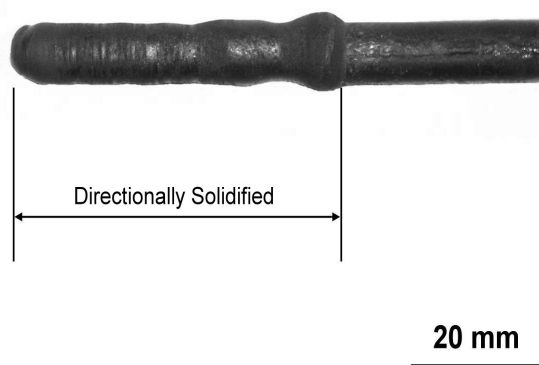


Figure 2 Cr-Ta samples directionally solidified at a growth speed of 40 mm/h and a rotation rate of 20 rpm.

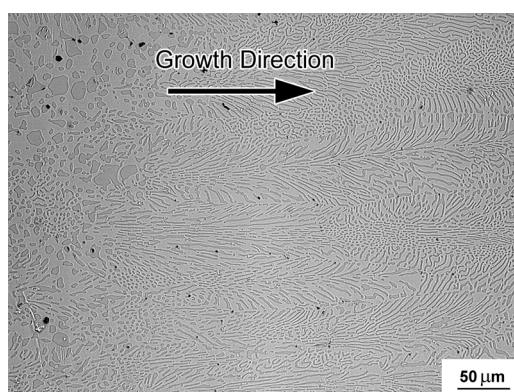


Figure 3 Longitudinal section of the DS Cr-Ta sample shown in Figure 2.

## 2. The DS microstructure in the binary Cr-Ta alloy

Figure 3 shows the longitudinal section of the DS Cr-9.6 at. %Ta alloy sample. The colony morphology of the eutectic structure indicates the instability of both the Cr-rich matrix and the  $\text{Cr}_2\text{Ta}$  phase. To obtain a well-aligned lamellar structure, the solid/liquid interface should be maintained planar and stable during the DS processing, which requires proper coupling of the composition of the molten alloy and the growth speed such that the undercooling at the solid/liquid interface is at an appropriate low level, thus, it is more feasible to obtain planar eutectic growth in alloys with near-eutectic compositions [28]. It is worth noting that the Ta concentration of 9.49 at. % Ta in the DS sample prior to DS (Table 2) was significant lower than the eutectic point of 9.7 at. % Ta in the Cr-Ta system [27]. For the DS processing employed in the present study, the composition of the molten alloy could be continuously varied during the growth due to the evaporation of Cr. Such a fluctuation on the order of 0.1 at. % Ta (as shown in Table 2) could become a serious obstacle to the development of well-aligned lamellar structures. Thus, a Cr-based alloy designed to be more tolerant to the composition deviations would be preferable for DS processing.

## 3. The eutectic composition of the Cr-Mo-Ta alloys

The eutectic Cr-9.7 at. % Ta alloy [27] was selected as the base composition for alloying with Mo, and various levels of Mo were added. Figure 4 summarizes the phase compositions of the drop-cast Cr-Mo-Ta alloys studied, and the typical OM microstructures are shown in Figure 5. It was found that the Mo addition at levels of 3.0 at. % and 5.0 at. % had significantly modified the eutectic point of the Cr-9.7 at. % Ta alloy, which led to a large amount of pro-eutectic dendrites throughout the microstructure [Figures 5(a) and 5(b)]. However, a fully eutectic structure was obtained in the samples with a lower Mo concentration of 1.0 at. %, as shown in Figures 5(c) and 5(d). A possible eutectic area is outlined in Figure 4.

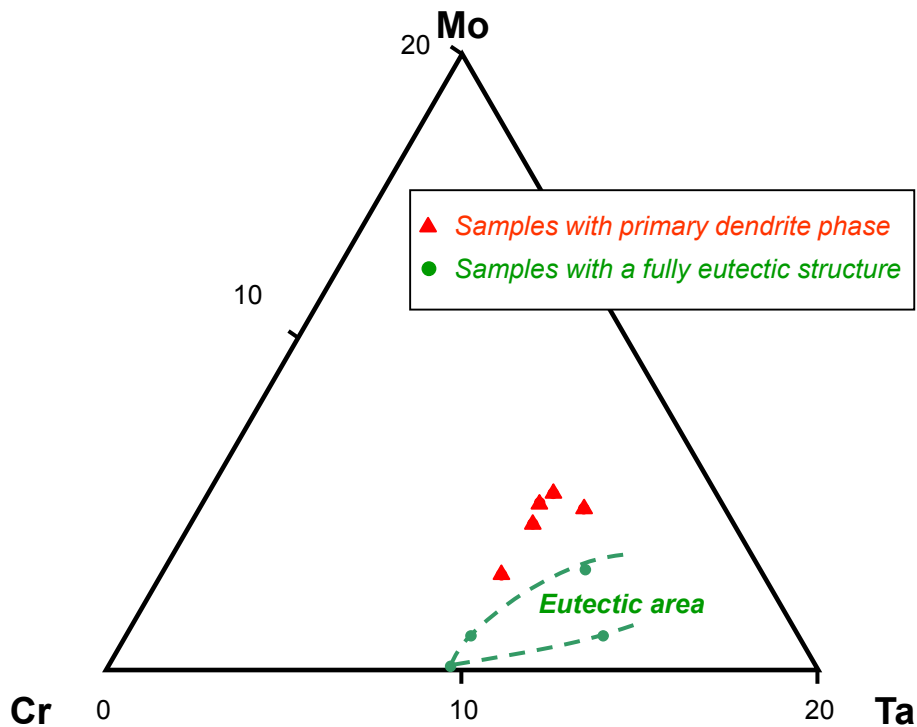


Figure 4 Phase composition of the Cr-Mo-Ta alloys studied, the axes are scaled in at. % .

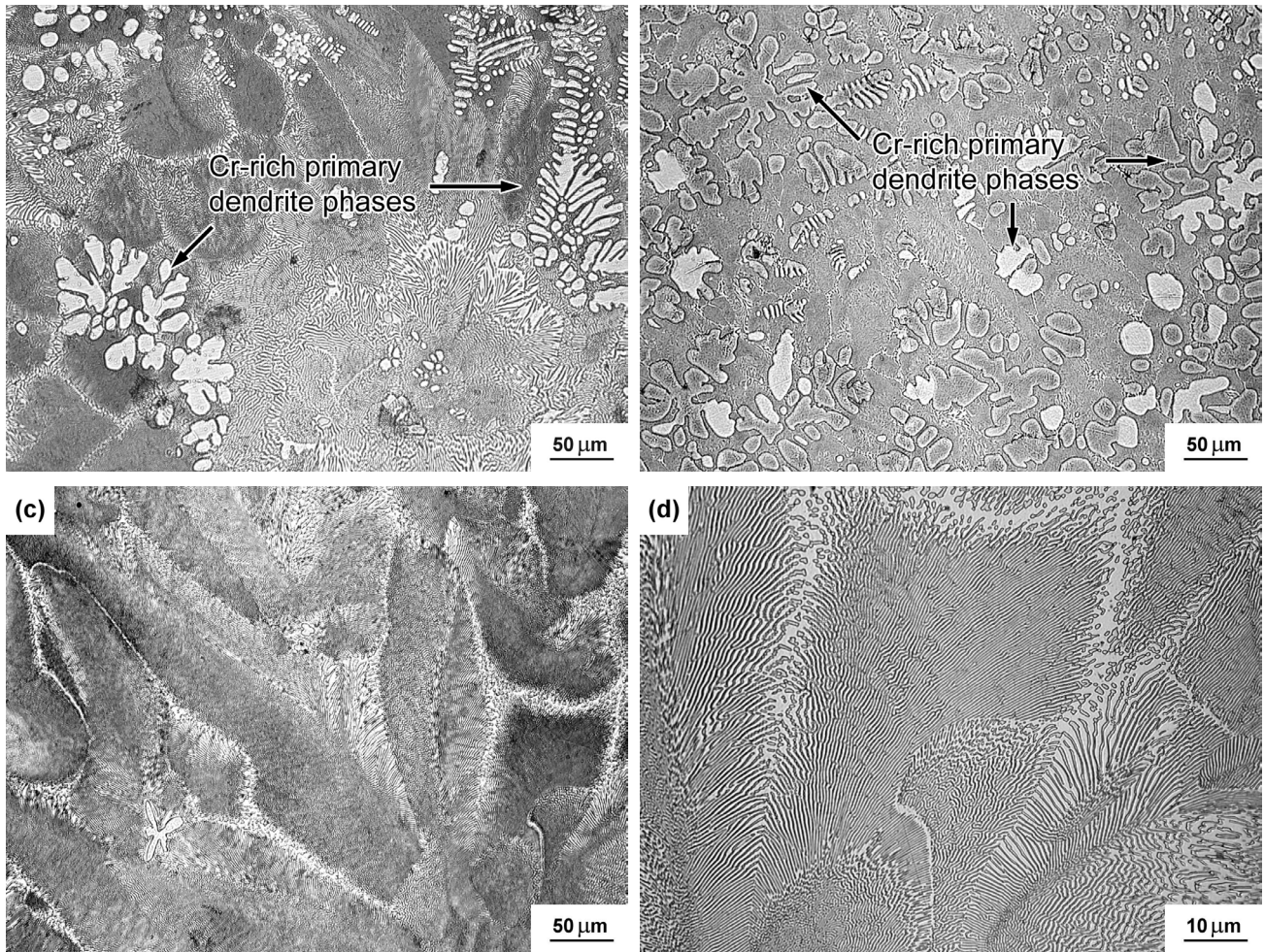


Figure 5 Optical micrographs of the drop-cast Cr-Ta-Mo alloys: (a) Cr-9.71 at. % Ta-5.01 at. % Mo; (b) Cr-9.67 at. % Ta-2.99 at. % Mo; (c) and (d) Cr-9.70 at. % Ta-1.00 at. % Mo.

### Summary

1. A quantitative tracking technique was developed to monitor and control the compositions of Cr-based alloys during processing at elevated temperatures. Evaporation of chromium was assumed to be the only source of the weight loss, which was carefully measured at each stage of processing, thus allowing the calculation and tracking of the compositions.
2. A colony structure related to the unstable liquid/solid interface was observed in a directionally-solidified Cr-Ta alloy with off-eutectic composition. The optimization of the growth parameters and alloy compositions is undergoing.
3. Ternary alloying with molybdenum was employed to improve the oxidization resistance and mechanical properties of the Cr-Ta alloys. It was found that there exists an eutectic area, which could tolerate the fluctuation in the alloy's composition during processing, and hence, facilitate the development of the lamellar structure in Cr-Mo-Ta alloys by directional solidification.

## Acknowledgment

The present research is sponsored by the Fossil Energy Advanced Research and Technology Development (AR&TD) Materials Program, U.S. Department of Energy, under subcontract No., 11X-SP173V, to the University of Tennessee, and by the AR&TD Materials Program, under contract No., DE-AC05-000R22725 with UT-Battelle, LLC. Dr. R. Judkins and Dr. P. Carlson are the contract monitors. One of the authors (DFW) thanks C.A. Carmichael, E. Lee, J.L. Wright, and Hongbin Bei for their kind help in the preparation and characterization of the alloys.

## References

1. Livingston J. D., Refractory and Silicide Laves Phases, in High-temperature silicides and refractory alloy, Briant C. L., Petrovic J. J., Bewlay B. P., Vasudevan A. K., and Lipsitt H. A., (eds.), Pittsburgh, MRS, 1994, 395-406.
2. Kumar K. S., Laves Phase-based Materials: Microstructure, deformation modes and properties, in high-temperature ordered intermetallic alloy, Koch C. C., Liu C. T., Stoloff N. S., and Wanner A., (eds.), Pittsburgh, MRS, 1997, 677-688.
3. Kumar K. S. and Liu C. T., Precipitation in a Cr-Cr<sub>2</sub>Nb alloy, *Acta Materialia*, **45**(1997), 3671-3686.
4. Ravichandran K. S., Miracle D. B., and Mendiratta M. G., Microstructure and mechanical behavior of Cr-Cr<sub>2</sub>Hf *in-situ* intermetallic composites, *Metallurgical and Materials Transactions*, **27**(1996), 2583-2592.
5. Zhu J. H., Liu C. T., and Liaw P. K., Phase stability and mechanical behavior of NbCr<sub>2</sub>-based Laves phase, *Intermetallics*, **7**(1999), 1011-1016.
6. Zhu J. H., Liu C. T., Pike L. M., and Liaw P. K., Thermodynamic interpretation of the size ratio limits for Laves phase formation, *Metallurgical and Materials Transaction*, **30**(1999), 1449-1452.
7. Zhu J. H., Pike L. M., Liu C. T., and Liaw P. K., Point defects in binary Laves phase alloys, *Acta Materialia*, **47**(1999), 2003-2018.
8. Zhu J. H., Pike L. M., Liu C. T., and Liaw P. K., Point defects in binary NbCr<sub>2</sub> Laves-phase alloys, *Scripta Materialia*, **39**(1998), 833-838.
9. Zhu J. H., Liaw P. K. and Liu C. T., Effect of electron concentration on the phase stability of NbCr<sub>2</sub>-based Laves phase alloys, *Materials Science and Engineering A*, **A240**(1997), 260-264.
10. Zhu J. H., Liu C. T., Pike L. M., and Liaw P. K., Enthalpies of formation of binary Laves phases, *Intermetallics*, **10**(2002), 579-595.
11. He Y. H., Liaw P. K., Lu Y., Liu C. T., Heatherly L., and George E. P., Effects of processing on the microstructure and mechanical behavior of binary Cr-Ta alloys, *Materials Science and Engineering A*, **A329**(2002), 696-702.
12. Brady M. P., Zhu J. H., Liu C. T., Tortorelli P. F., and Walker L. R., Oxidation resistance and mechanical properties of Laves phase reinforced Cr *in-situ* composites, *Intermetallics*, **8**(2000), 1111-1118.
13. Aoyama N. and Hanada S., Microstructure and strength of NbCr<sub>2</sub>/Cr composites, *Materials Transaction - JIM*, **38**(1997), 155-162.
14. Reviere R., Sauthoff G., Jonson D. R., and Oliver B. F., Microstructure of directionally solidified eutectic based Fe(Al, Ta)/Fe<sub>2</sub>Ta(Al) alloys as a function of processing condition, *Intermetallics*, **5**(1997), 161-172.
15. Liu C. T., Tortorelli P. F., Horton J. A., and Carmichael C. A., Effects of alloy additions on the microstructure and properties of Cr-Cr<sub>2</sub>Nb alloys, *Materials Science and Engineering A*, **A214**(1996), 23-32.
16. Bewlay B. P. and Jackson M. R., Effect of Hf and Ti additions on microstructure and properties of Cr<sub>2</sub>Nb-Nb *in situ* composites, *Journal of Materials Research*, **11**(1996), 1917-1922.
17. Takeyama M. and Liu C. T., Microstructure and mechanical properties of Laves phase alloys based on Cr<sub>2</sub>Nb,

*Materials Science and Engineering A*, **A132**(1991), 61-66.

18. Kumar K. S., Pang L., Liu C. T., Horton J., and Kenik E. A., Structural stability of the Laves phase  $\text{Cr}_2\text{Ta}$  in a two-phase  $\text{Cr-Cr}_2\text{Ta}$  alloy, *Acta Materialia*, **48**(2000), 911-923.
19. Tagasugi T., Kumar K. S., Liu C. T., and Lee E. H., Microstructure and properties of two-phase  $\text{Cr-Cr}_2\text{Nb}$ ,  $\text{Cr-Cr}_2\text{Zr}$  and  $\text{Cr-Cr}_2(\text{Nb, Zr})$  alloys, *Materials Science and Engineering A*, **A260**(1999), 108-123.
20. Brady M. P., Zhu J. H., Liu C. T., Tortorelli P. F., Walker L. R., McKamey C. G., and Wright J. L., Intermetallics reinforced Cr Alloy for high-temperature use, *Materials at High Temperatures*, **16**(1999), 189-193.
21. Massalski T. B., Murray J. L., Bennett L. H., and Baker H. (eds.), Binary alloy phase diagram, American Society for Metals, Metals Park, OH, 1986, 867.
22. Matsumoto Y., Fukumori J., Morinaga M., Furui M., Nambu T., and Sakaki T., Alloying effect of 3D transition elements on the ductility of chromium, *Scripta Materialia*, **34**(1996), 1685-1689.
23. Provenzano V., Valiev R., Rickerby D. G., and Valdre G., Mechanical properties of nanostructured chromium, *Nanostructured Materials*, **12**(1999), 1103-1108.
24. Morinaga M. and Nambu T., Effect of surface imperfections on the ductility of pure chromium, *Journal of Materials Science*, **30**(1995), 1105-1110.
25. He Y. H., Wang D. F., Liaw P. K., Liu C. T., Heatherly L., and George E. P., Processing, microstructure and mechanical properties of the  $\text{Cr-Ta}$  composites reinforced by the  $\text{Cr}_2\text{Ta}$  Laves phase, 15<sup>th</sup> Annual Conference on Fossil Energy Materials, Knoxville, Tennessee, 2001.
26. Liu C. T., Zhu J. H., Brady M. P., McKamey C. G., and Pike L. M., Physical metallurgy and mechanical properties of transition-metal Laves phase alloy, *Intermetallics*, **8**(2000), 1119-1129.
27. Wang D. F., Liaw P. K., Liu C. T., Heatherly L., and George E. P., Processing and microstructures of  $\text{Cr-Ta}$  and  $\text{Cr-Ta-Mo}$  composites reinforced by  $\text{Cr}_2\text{Ta}$  Laves phase, TMS 2003 132<sup>nd</sup> TMS Annual Meeting, San Diego, California, 2003
28. Kurz W. and Fisher D.J., Fundamentals of solidification, Trans Tech Publications, 1984